Properties of Transient K^+ Currents and Underlying Single K^+ Channels in Rat Olfactory Receptor Neurons

JOSEPH W. LYNCH and PETER H. BARRY

From the School of Physiology and Pharmacology, University of New South Wales, Sydney, New South Wales 2033, Australia

ABSTRACT The transient potassium current, $I_K(t)$, of enzymatically dissociated rat olfactory receptor neurons was studied using patch-clamp techniques. Upon depolarization from negative holding potentials, $I_K(t)$ activated rapidly and then inactivated with a time course described by the sum of two exponential components with time constants of 22.4 and 143 ms. Single-channel analysis revealed a further small component with a time constant of several seconds. Steady-state inactivation was complete at −20 mV and completely removed at −80 mV (midpoint −45 mV). Activation was significant at −40 mV and appeared to reach a maximum conductance at +40 mV (midpoint −13 mV). Deactivation was described by the sum of two voltage-dependent exponential components. Recovery from inactivation was extraordinarily slow (50 s at −100 mV) and the underlying processes appeared complex. $I_K(t)$ was reduced by 4-aminopyridine and tetraethylammonium applied externally. Increasing the external K^+ concentration ($[K^+]_o$) from 5 to 25 mM partially removed $I_K(t)$ inactivation, usually without affecting activation kinetics. The elevated $[K^+]_o$ also hyperpolarized the steady-state inactivation curve by 9 mV and significantly depolarized the voltage dependence of activation. Single transient K^+ channels, with conductances of 17 and 26 pS, were observed in excised patches and often appeared to be localized into large clusters. These channels were similar to $I_K(t)$ in their kinetic, pharmacological, and voltage-dependent properties and their inactivation was also subject to modulation by $[K^+]_o$. The properties of $I_K(t)$ imply a role in action potential repolarization and suggest it may also be important in modulating spike parameters during neuronal burst firing. A simple method is also presented to correct for errors in the measurement of whole-cell resistance (R_o) that can result when patch-clamping very small cells. The analysis revealed a mean corrected R_o of 26 GΩ for these cells.

INTRODUCTION

Interaction between odorants and olfactory receptor neurons results in depolarizing receptor potentials which activate voltage-gated channels and generate bursts of spikes. The voltage-gated currents underlying the excitatory response form an

Address reprint requests to Dr. Peter H. Barry, School of Physiology and Pharmacology, University of New South Wales, P.O. Box 1, Kensington, NSW 2033, Australia.

J. GEN. PHYSIOL. © The Rockefeller University Press · 0022-1295/91/05/1043/30 $2.00
Volume 97 May 1991 1043–1072

important part of the olfactory transduction process and have been investigated in a number of laboratories. Whole-cell currents have been studied in the olfactory cells of lobsters (McClintock and Ache, 1989) and a variety of amphibian species (Trotier, 1986; Firestein and Werblin, 1987*a*; Dionne, 1989; Schild, 1989; Suzuki, 1989; Trotier et al., 1989). Some of the underlying single channels have been studied in lobster (McClintock and Ache, 1989), salamander (Trotier, 1986), and mouse (Maue and Dionne, 1987*a*) olfactory receptor neurons. These studies have revealed several types of K^+ channels, separated on the basis of different voltage, kinetic, and pharmacological sensitivities. Transient K^+ currents activated by depolarization were reported in a minority of studies (Firestein and Werblin, 1987*a*; Schild, 1989; Trotier et al., 1989) and have not been described in detail. As in many other types of neurons, this current is difficult to isolate from the delayed rectifier over a wide range of membrane potentials and this may have prevented detailed characterization.

We have found that rat olfactory receptor neurons express large transient K^+ currents, and because the delayed rectifier is frequently absent, detailed analysis has been possible. In this paper we present a description of the transient K^+ current, $I_K(t)$, and its underlying single channels. The properties revealed by this analysis are consistent with the limited information available from other species and indicate that $I_K(t)$ may be important in spike repolarization. Other characteristics suggest that it may also be responsible for the progressive modification of action potential parameters during neuronal burst firing.

We have previously presented evidence that the whole-cell resistance of rat olfactory receptor neurons is ~40 GΩ (Lynch and Barry, 1989). Although the whole-cell patch configuration is indispensable for studying the membrane properties of small cells, it cannot be used to directly measure the whole-cell resistance or resting potential of cells where the input resistance is greater than or similar in magnitude to the pipette-membrane seal resistance (which is typically 10–50 GΩ). We describe a simple means of overcoming this problem, which relies on the assumption that the resting conductance is carried exclusively by K^+ ions. The analysis indicated a whole-cell resistance of 20–30 GΩ for these cells, which is in reasonable agreement with our earlier result.

METHODS

Cell Preparation

The method of producing enzymatically dissociated rat olfactory receptor neurons was based on that described by Maue and Dionne (1987*b*). Adult Wistar rats were killed by CO_2 inhalation. Olfactory epithelia and supporting cartilage were quickly removed and placed in divalent cation-free Dulbecco's phosphate-buffered saline (DPBS). Epithelia were then gently separated from the cartilage, dissected into small pieces, and rinsed with two changes of solution. The tissue pieces were then placed in 5 ml of DPBS containing 0.022% trypsin (Calbiochem-Behring Corp., La Jolla, CA) and incubated for 35 min at 37°C. The dissociation was terminated by removing the dissociation solution and replacing it by 10 ml of general mammalian Ringer's (GMR) solution. Then, by applying gentle trituration with a fire-polished pipette, large numbers of olfactory cells were isolated. Approximately 2 ml of supernatant was pipetted onto a glass coverslip on the bottom of a flow-through recording chamber. The coverslip had previously been coated with concanavalin A (Maue and Dionne, 1987*b*) to permit cell adhesion.

The preparation was viewed at ×400 with an inverted microscope (model IMT-2, Olympus Corp., Tokyo, Japan) using phase-contrast optics. Although several cell types were isolated, olfactory receptor neurons were readily identified by their characteristic bipolar morphology (Maue and Dionne, 1987*b*) and the ability to fire action potentials. Short villi protruding from the dendritic knob were visible in a minority of neurons. On others the presence of longer, finer cilia was frequently suggested but not clearly resolved by our microscope optics. No consistent differences were noted in the ionic currents of either type. Neurons isolated by these procedures were small (5–8 μm diam) and remained viable for 5–6 h.

Data Recording

The inside-out, outside-out, and whole-cell configurations of the patch-clamp technique were used (Hamill et al., 1981). Patch pipettes were made from borosilicate haematocrit tubing (Modulohm 1/S, Vitrex, Herlev, Denmark) and coated with Sylgard (No. 170, Dow Corning Corp., Midland, MI) to within 50 μm of the tip. When fire-polished and filled with saline, pipettes had tip resistances of 2–5 MΩ.

The whole-cell recordings were obtained using standard procedures. Series resistance compensation was often employed but appeared to be unnecessary as its application or removal seldom had any effect on the speed of the voltage-clamp or the magnitude of peak currents. Similar observations have been made by others using very small cells (e.g., Deutsch et al., 1986). Unstimulated cells were voltage-clamped at −80 mV and digitally generated test pulses were applied at 5-s intervals.

The inside-out patch configuration was routinely achieved by subjecting cell-attached patches to brief air exposure. However, the formation of outside-out patches from whole-cell seals was seldom successful by either this or any other method. Excised membrane patches were usually transferred to a separate chamber as previously described (Lynch et al., 1988) where multiple rapid solution exchanges could be performed. Patch transfer success rates were virtually 100% with this preparation.

Currents were recorded using an EPC-7 patch-clamp amplifier (List Medical, Darmstadt, FRG). Data were filtered at 10 kHz and recorded on videotape. Experiments were performed at room temperature (20–22°C).

Solutions

The cells were bathed in GMR, which contained (in mM) NaCl 140, KCl 5, $MgCl_2$ 1, $CaCl_2$ 2, Na *N*-2-hydroxyethylpiperazine-*N'*-2-ethanesulfonic acid (HEPES) 10, glucose 10 (pH 7.2). In most whole-cell experiments Na^+ was replaced by choline. In experiments using 25 mM $(K^+]_o$, choline concentration was reduced to maintain osmolality. In various experiments, tetrodotoxin (TTX, 0.1–7 μM), 4-aminopyridine (4-AP, 1–5 mM), tetraethylammonium chloride (TEACl, 1–5 mM), $CoCl_2$ (2 mM), and $CdCl_2$ (0.1–1 mM) were added directly to the bathing solution and, if necessary, the pH was readjusted to 7.2. The pipette solution for whole-cell experiments contained (in mM): KF 125, KCl 15, ethyleneglycol-bis-(β-amino-ethyl ether)*N,N'*-tetra-acetic acid (EGTA) 11, K-HEPES 10 (pH 7.2). Similar pipette and bathing solutions were used for outside-out single-channel recordings.

For inside-out single-channel recordings, the pipette contained either GMR or a high $[K^+]_o$ solution consisting of (in mM) KCl 145, $MgCl_2$ 1, $CaCl_2$ 2, K-HEPES 10, glucose 10 (pH 7.2). Inside-out patches were exposed to either GMR or a high $[K^+]_i$ solution which contained (in mM) KCl 145, $MgCl_2$ 2, $CaCl_2$ 1, K-HEPES 10, glucose 10 (pH 7.2). In some experiments, $[Ca^{++}]_i$ was reduced to 0.1 μM. In this case, the external solution contained (in mM): KCl 145, $MgCl_2$ 2, $CaCl_2$ 0.045, EGTA 0.08, K-HEPES 10, glucose 10 (pH 7.2), similar to that reported by Barrett et al. (1982).

Most reagents were obtained from Sigma Chemical Co, St Louis, MO, with the exception of TEACl (Merck, Munich, FRG), HEPES (Calbiochem-Behring Corp.) and $CdCl_2$ (BDH Chemicals, Poole, England).

Data Analysis and Display

Whole-cell current data were filtered at 2 kHz, digitised at 5 kHz and analyzed on an IBM-AT computer using PNSCROLL software (Barry and Quartararo, 1990). Leakage currents were small and were compensated as described in the legend to Fig. 2 *C*. Data displayed below (except Fig. 3) were not corrected for leakage or capacitative currents. Single-channel data were filtered at 1 kHz, digitized at 5 kHz, and analyzed as above. Capacitative transients and nonlinear baselines induced by voltage steps were compensated by digitally subtracting many averaged blank or subthreshold traces to the same potential. Voltages are expressed as the potential of the interior with respect to the exterior membrane surface. In all figures, upward deflections represent current flow out of the cell, or from the internal to the external membrane surfaces of excised patches.

All voltages have been corrected for liquid junction potentials (LJPs) as described in detail elsewhere (Barry and Lynch, 1991). Briefly, in all experiments the pipette offset potential was nulled when the bath contained GMR and the ground was provided by a Ag/AgCl electrode gelled in 150 mM KCl. After establishment of the whole-cell seal, the bath solution was exchanged for choline Ringer's. The LJP between the KF pipette solution and GMR was −8.5 mV, and between the choline Ringer's and the KCl electrode was +9.0 mV. Thus, under our recording conditions these potentials virtually cancelled leaving no correction necessary. However, the LJP between the KF pipette solution and choline Ringer's was −12.5 mV, a quantity which is important when estimating whole-cell resistance (see below).

RESULTS

Passive Cell Properties

Cells had an average zero-current potential of −52 ± 4 mV (mean ± SEM, n = 9, range −40 to −73 mV), which was similar to that recently reported in cultured rat olfactory receptor neurons (Pixley and Pun, 1990). Superimposed upon the zero-current potential were irregular rapid voltage fluctuations (typically up to ± 10 mV) apparently caused by the random opening and closing of ionic channels. Cells with zero-current potentials more positive than −30 mV generally had significant linear leakage currents and were not studied. We have previously presented evidence that the whole-cell resistance (R_o) in rat olfactory neurons is ~40 GΩ (Lynch and Barry, 1989). Since the pipette-membrane seal resistance (R_s) is of a similar magnitude, it represents a low-resistance pathway to ground for currents responsible for maintaining cell resting potential. Accordingly, cell resting potentials are underestimated when determined by this method.

Similarly, R_o is underestimated when determined by measuring the current required to produce a given change in membrane potential, because a significant proportion of current is shunted across R_s. A simplified electrical circuit is shown in Fig. 1 *A*. The pipette potential and the normal cell resting membrane potential are given by V_p and E_m, respectively. E_s is the potential across the pipette-membrane seal resistance. It is assumed to be nonselective and represents only the LJP between internal (pipette) and external solutions. The amplifier is indicated by "A." From this

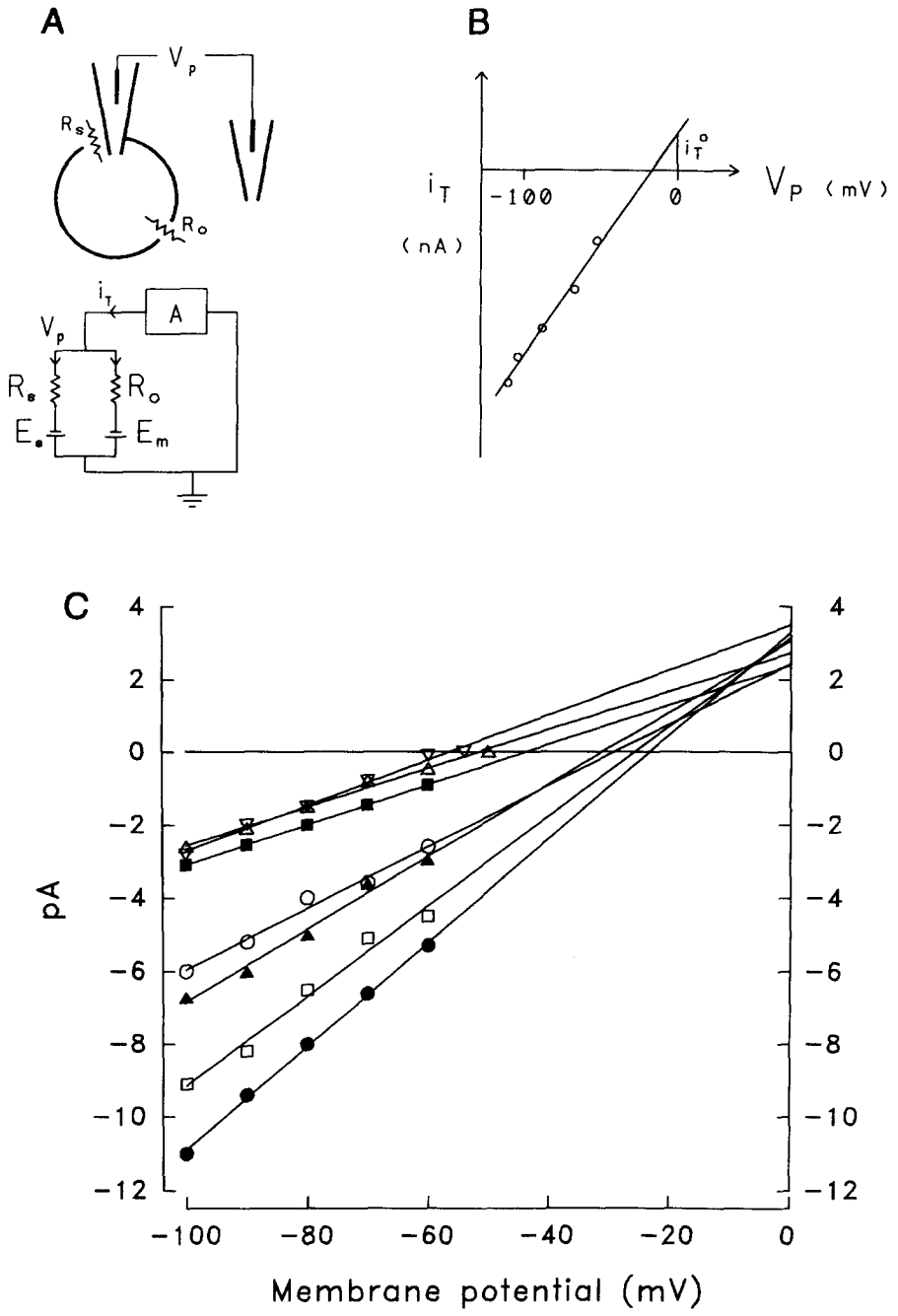

FIGURE 1. Estimation of whole-cell resistance. (*A*) A schematic diagram of the whole-cell configuration (*upper panel*) and a simplified circuit diagram of the electrical situation (*lower panel*). Parameters are as follows: R_o, whole-cell resistance; R_s, pipette-membrane seal resistance; E_s, liquid junction potential across R_s; E_m, cell resting membrane potential; V_p, pipette potential; and i_T, total current measured by the amplifier. "A" represents the amplifier. (*B*) Graphical representation of Eqs. 2 and 3, indicating the method of estimating R_o. The *I-V* relationship in the voltage range of interest is plotted and projected to the point where $V_p = 0$, allowing measurement of i_t^o and $\Delta i_T/\Delta V_P$. Using these quantities and other appropriate assumptions (see text), R_o can be found by solving Eqs. 2 and 3. (*C*) The current required to hold the cell at potentials from −60 to −100 mV is plotted for seven cells. Points were fitted by linear regression and were extrapolated to the point where $V_p = 0$. These data were used to estimate a mean R_o of 26 GΩ.

circuit, the total current (i_T) measured by the amplifier is:

$$i_T = (V_p - E_s)/R_s + (V_p - E_m)/R_o. \quad (1)$$

If the cell current–voltage (I-V) relationship measured over the voltage range of interest is extrapolated to the point where $V_P = 0$ (Fig. 1 *B*), then the corresponding current (i_T^o) is given by:

$$i_T^o = - E_s/R_s - E_m/R_o. \quad (2)$$

The slope of the I-V relationship (Fig. 1 *B*) is given by:

$$\Delta i_T/\Delta V_P = 1/R_s + 1/R_o. \quad (3)$$

$\Delta i_T/\Delta V_P$ and i_T^o can be measured as shown in Fig. 1 *B*. Since the liquid junction potential (E_s) can be measured or calculated and E_m is assumed to be equal to the K^+ equilibrium potential, both R_o and R_s can be calculated by simultaneously solving Eqs. 2 and 3. Note that this analysis relies on the assumptions that the resting K^+ conductance is carried by K^+ ions (see Discussion) and that E_s represents only a nonselective LJP.

To test this model, the membrane potential was stepped from −60 to −100 mV in 10-mV increments at 2-s intervals while monitoring the holding current. No ionic currents were gated by this procedure and I-V relationships were usually linear in this range. E_s was calculated to be −12.5 mV (Barry and Lynch, 1990). Data from seven cells are plotted in Fig. 1 *C* and indicate an R_o of 26.1 ± 1.8 GΩ (mean ± SEM, range 18.9–30.9 GΩ). R_o generally declined dramatically at potentials more positive than −55 mV.

Whole-cell capacitative transients in response to 3-mV hyperpolarizing voltage pulses were minimized when the amplifier slow capacitative compensation was set between 2 and 4 pF. We previously determined a whole-cell capacitance (C_o) of 3 pF by a different method (Lynch and Barry, 1989).

Isolation of the Transient K^+ Current

When sufficiently large depolarizing voltage steps from a holding potential of −88 mV were applied to cells bathed in GMR, rapid inward currents followed by inactivating outward currents were always observed (Fig. 2 *A*). Replacement of external Na^+ by choline selectively abolished the inward current (Fig. 2 *B*). The addition of TTX (0.1–7.0 μM) to the normal bath solution blocked a varying fraction of this current, but seldom all of it.

Whole-cell Ca^{++} currents or Ca^{++}-activated K^+ currents were not observed, although single-channel investigations in this preparation have revealed the presence of both types (Maue and Dionne, 1987*a*; Lynch and Barry, unpublished observation). The addition of the Ca^{++} channel blocker Co^{++} (2 mM) to the bath solution had negligible effects on inward or outward currents. It appears that F^- ions in the pipette may have inactivated the Ca^{++} current (Kostyuk et al., 1975) and that this, coupled with strong chelation of internal Ca^{++} ions by internal EGTA, may have precluded activation of the Ca^{++}-activated K^+ current. Cadmium (1 mM) was not useful as a Ca^{++} channel blocker as it directly suppressed and delayed the activation

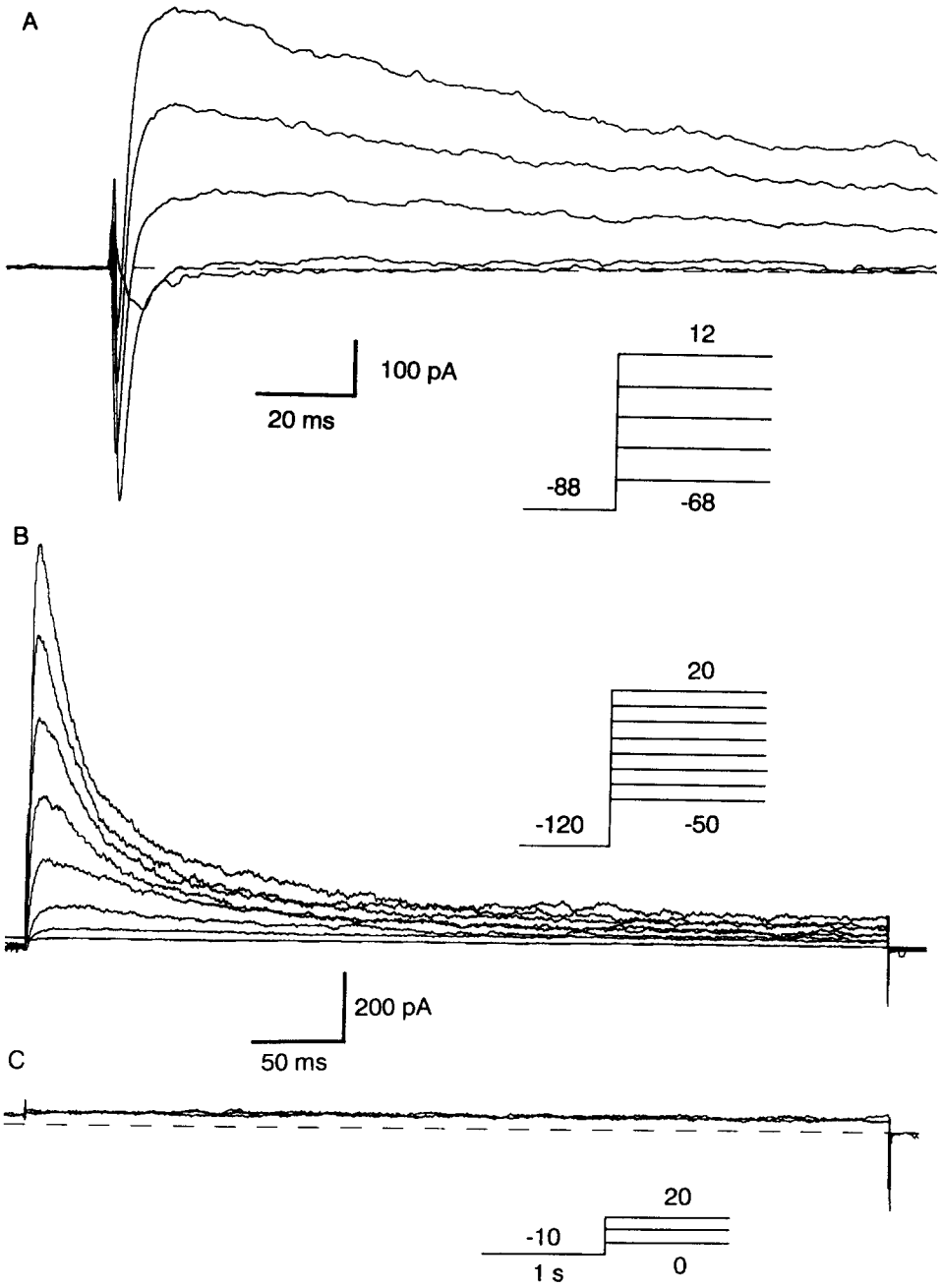

FIGURE 2. Whole-cell currents activated by depolarization from negative membrane potentials. Dashed lines are drawn through the steady-state current level at −80 mV. (*A*) Currents activated by depolarization from −88 mV to potentials between −68 and +12 mV (in 20-mV increments). The pipette contained KF solution and the bath contained GMR. (*B*) Currents activated by depolarization from −120 mV (2 s) to potentials between −50 and +20 mV (in 10-mV increments) in another cell where external Na^+ was replaced by choline. (*C*) Currents activated at potentials of 0, 10, and 20 mV in the same cell after 1-s prepulses to −10 mV. The transient current shown in *B* was completely inactivated. Leakage subtraction for data analysis was performed by subtracting these traces from the corresponding traces in *B*. For potentials ≤ −10 mV, leakage was estimated by linearly extrapolating the 0 mV mean leakage current to zero at −50 mV.

of the transient K^+ current (Fig. 3). It also caused a depolarizing shift of ~10 mV in the voltage dependence of steady-state inactivation.

The outward current, which was carried by K^+ ions, activated rapidly and inactivated almost completely within 500 ms (Fig. 2 *B*). The transient component of this current has been designated $I_K(t)$. A few cells also expressed a small, slowly activating delayed rectifier, $I_K(dr)$, which was difficult to isolate from $I_K(t)$. Low concentrations of TEA blocked $I_K(dr)$ (not shown) and reduced $I_K(t)$ (Fig. 3). Although 4-AP suppressed $I_K(t)$ (Fig. 3), its effect was incomplete and the residual current usually swamped $I_K(dr)$. Both currents also activated over similar voltage ranges and both displayed steady-state inactivation. However, a 1-s conditioning step to −10 mV completely inactivated $I_K(t)$ (Fig. 2 *C*), but only partially inactivated $I_K(dr)$, which could then be detected by stepping to more positive potentials. Cells expressing significant delayed rectifier currents when isolated by this procedure were excluded from analysis.

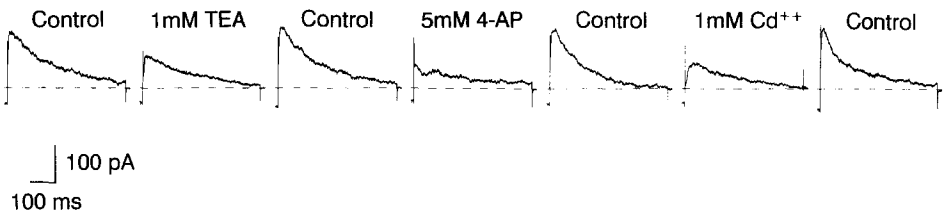

FIGURE 3. Pharmacology of $I_K(t)$. Result of the successive application of 1 mM TEA, 5 mM 4-AP, and 1 mM Cd^{++} to the same cell bathed in choline Ringer's solution. Effects of TEA and 4-AP were easily reversed but Cd^{++} required a more extensive washout. Currents were recorded at −10 mV after depolarization from −120 mV. These records were corrected for leakage by subtracting the response after a subthreshold depolarization (−20 mV to −10 mV) from each trace.

Whole-cell analysis of $I_K(t)$ was performed in the presence of external choline. $I_K(t)$ usually decreased in size and underwent an ~−10-mV shift in voltage dependence within the first 5 min of whole-cell recording. Recordings were commenced after this period. The average $I_K(t)$ conductance in 11 cells was 6.8 ± 1.1 nS (mean ± SEM).

Time and Voltage Dependence of $I_K(t)$ in 5 mM $(K^+]_o$

In response to sustained depolarizations to potentials between −40 and +40 mV, currents inactivated with a time course that was well described by the sum of two exponential components. The time constants of these components were found by the "exponential peeling" technique, as displayed in Fig. 4 *A*. At potentials > −30 mV, both components were always present and most of the current inactivated via the rapid process. The faster time constant displayed a voltage-dependent increase at potentials < −20 mV. At potentials more positive to this, the mean inactivation time constants were 22.4 ± 1.0 and 143 ± 8 ms (both ± SEM, n = 25), respectively. A recent report (Cooper and Shrier, 1989) presented evidence for a third, longer decay time constant (3–11 s) in A currents from rat nodose neurons. However, such a long

time-constant component appeared to account for < 5% of the total $I_K(t)$ inactivation.

Upon step depolarization of the cell membrane, currents activated rapidly. The time to half-maximal activation was measured for currents activated to between −30 and +40 mV. It was found to be voltage-dependent and reached a minimum of 1.46 ± 0.06 ms (mean ± SEM, n = 7) at 40 mV (Fig. 4 *B*, ○ and ●). There was essentially no difference in the times measured in 5 mM $[K^+]_o$ (Fig. 4 *B*, ●) or 25 mM $[K^+]_o$ (○), although as it will be shown below, increasing $[K^+]_o$ significantly delayed inactivation and deactivation kinetics. Although the time-to-peak-current activation was slightly prolonged in elevated $[K^+]_o$, this was probably due to the modification of inactivation, rather than activation, kinetics.

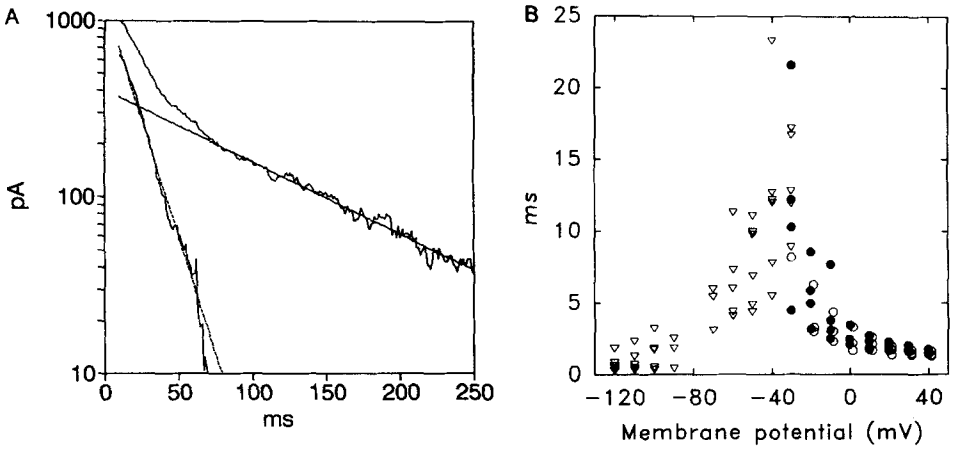

FIGURE 4. Kinetics of $I_K(t)$. (*A*) Inactivation of $I_K(t)$ is described by the sum of two exponential components. The trace for +20 mV in Fig. 2 *B* was replotted on semilogarithmic axes (*upper curve*). A straight line was fitted to the straight part of the curve by linear regression (*solid line*). This was subtracted from the original trace leaving a steeper trace which was fitted by a similar procedure (*dashed line*). The solid line represents the slow inactivation time constant (108 ms) and the dashed line represents the rapid inactivation time constant (17.5 ms). Most of the current inactivated by the rapid process. (*B*) Time to one-half activation (*circles*) and time to one-half deactivation of tail currents (*triangles*). There was no difference in activation data from four cells bathed in 5 mM $[K^+]_o$ (●) or from three cells bathed in 25 mM $[K^+]_o$ (○). Time to one-half deactivation (▽) was measured in six cells in 5 mM $[K^+]_o$.

Deactivation of $I_K(t)$ was determined by measuring the time to half-decay of tail currents recorded between −30 and −120 mV after a 10-ms activating prepulse to −10 mV (e.g., see Fig. 7 *A*). Times to half-decay, plotted for five cells, are displayed in Fig. 4 *B* (▽). Although there was considerable variation between cells, the half-times for any given cell were highly voltage dependent. Tail current decay profiles were generally described by the sum of two exponential components, both of which increased with $[K^+]_o$ (see below).

The steady-state inactivation curve was investigated by holding the membrane potential for 1 s at conditioning steps from −20 to −120 mV (10-mV increments) and

then measuring the maximum current available upon stepping to −10 mV. Membrane potential was maintained at −120 mV for 5 s between tests. A result from one cell is shown in Fig. 5 *A*. Data from five such cells are plotted in Fig. 5 *B* (■). Currents were completely reactivated at potentials more negative than −80 mV and were almost completely inactivated at potentials more positive than −20 mV. The steady-state inactivation curve was approximated by a Boltzmann type distribution:

$$G = 1/[1 + \exp[(V' - V)/k]], \quad (4)$$

where G is the relative maximum conductance, V is the membrane potential of the conditioning pulse, V' is the potential corresponding to the midpoint of inactivation, and k is the slope factor. The fitted curve was obtained when V' and k were −45 and −8 mV, respectively.

Channel activation was determined by measuring the maximum current available at potentials ranging from −70 to +40 mV, when stepped from a holding potential of −100 or −120 mV. The peak conductance at each potential was calculated assuming perfect K^+ selectivity and expressed as a fraction of the conductance at +40 mV. Fig. 5 *B* (□) displays activation data averaged from five cells. Activation was significant at −40 mV and appeared to reach a maximum near +40 mV. Activation kinetics were also described by a Boltzmann distribution (see Eq. 4), where V' is now the potential corresponding to the midpoint of activation. The fitted curve was obtained when V' and k were −13 and 11 mV, respectively.

Recovery from inactivation of $I_K(t)$ required an unusually long time and the underlying kinetic processes appeared complex. Both characteristics resembled those recently reported for the inactivating K^+ current in clonal pituitary (GH_3) cells (Oxford and Wagoner, 1989). Recovery was investigated in 5 mM $[K^+]_o$ at four different holding potentials (−80, −100, −120, and −140 mV) by the voltage protocol illustrated in Fig. 6. Inactivation was considered to be fully removed by a 2-s hyperpolarizing voltage step to −140 mV. The magnitude of the current that was then activated by stepping to −10 mV was used as a measure of the fully reactivated state. The potential, after being maintained at −10 mV for 1 s to ensure complete inactivation, was returned to the holding potential for varying periods of time and then stepped back to −10 mV. The current that had recovered from inactivation was compared to the initial peak current. Results obtained from a total of six cells were normalized and are plotted in Fig. 6 (note the logarithmic time scale). The recovery rate was strongly voltage dependent but tended to converge at increasingly negative holding potentials. As noted by Oxford and Wagoner (1989), the voltage dependence of recovery was most obvious at the briefest interpulse intervals, suggesting that most of the voltage dependence resided in the fastest part of the recovery process.

Effect of Increasing $[K^+]_o$

The ionic selectivity of $I_K(t)$ was investigated by measuring the reversal potential of tail currents in choline Ringer's solution containing the normal concentration (5 mM) of K^+ ions. Outward current was activated by a 10-ms depolarizing pulse to −10 mV, then stepped to potentials from −20 to −110 mV (10-mV increments). In a typical result shown in Fig. 7 *A*, tail currents reversed near the K^+ equilibrium potential of −82 mV. The mean reversal potential in five cells was −79 ± 2 mV (mean ± SEM),

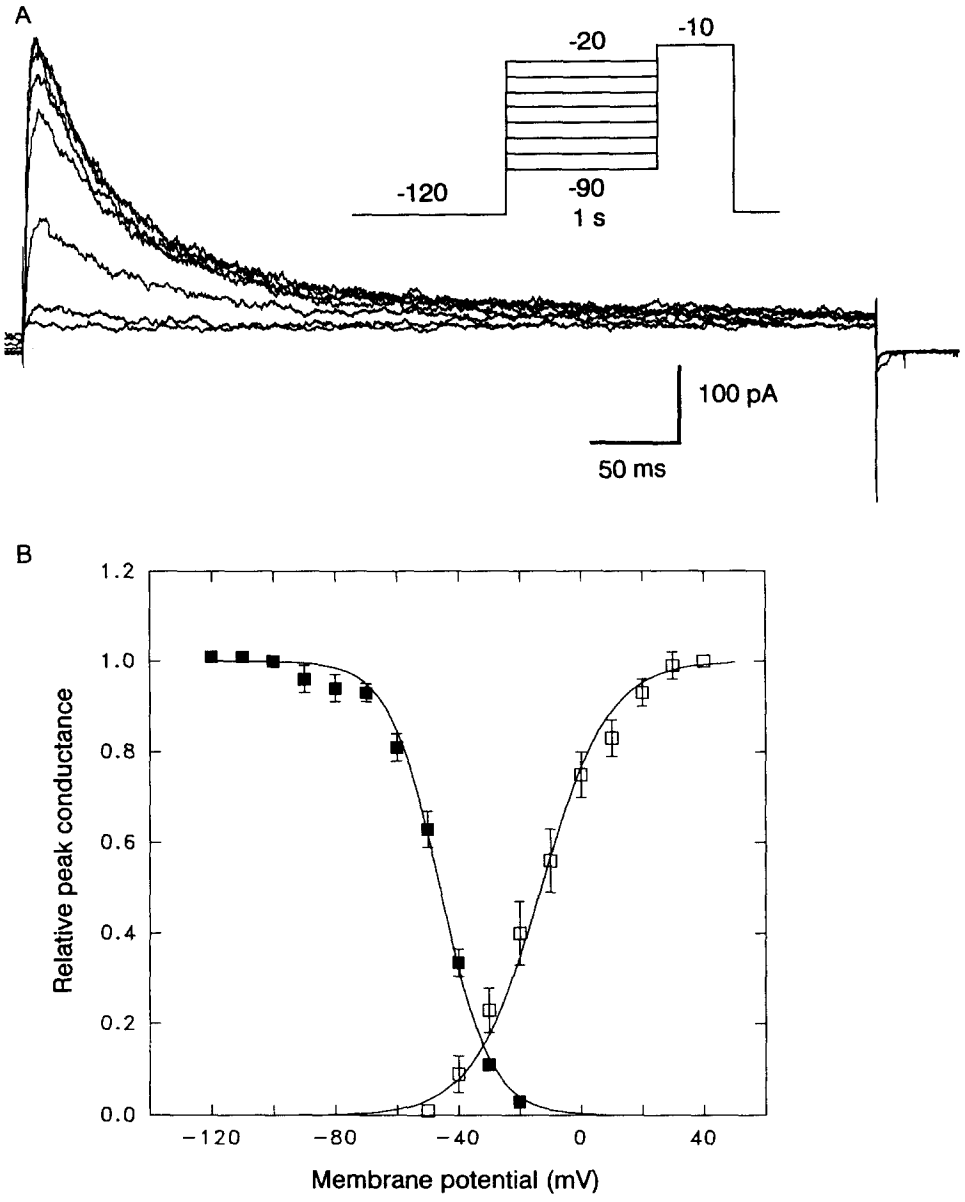

FIGURE 5. Steady-state inactivation and voltage-dependent activation of $I_K(t)$. (*A*) Example of steady-state inactivation data recorded from one cell by the voltage protocol illustrated in the inset. (*B*) Steady-state inactivation (■) and activation data (□) were both averaged from five cells. Error bars (± SEM) are displayed when larger than symbol size. Steady-state inactivation conductance was expressed as a fraction of that activated by depolarization from −100 mV. Peak activation conductances were expressed as a fraction of those measured at +40 mV. In each case, Boltzmann distributions (*solid lines*) were fitted by eye. See text for parameters of best fit.

suggesting that K^+ was the predominant charge carrier for this current. The experiment was repeated in the same five cells after raising $[K^+]_o$ to 25 mM. This shifted the K^+ equilibrium potential to −42 mV. Tail currents reversed at −38 ± 2 mV (mean ± SEM) (e.g., Fig. 7 *B*), providing further evidence for K^+ ions being the main charge carriers through these channels.

It is obvious from Fig. 7 that the increased $[K^+]_o$ had the additional effect of greatly reducing the rate of tail current deactivation. This effect was reversible and was observed in each of the five cells studied. It was considered most likely due to either (*a*) activation of an otherwise covert K^+ current by external K^+ ions or (*b*) removal of

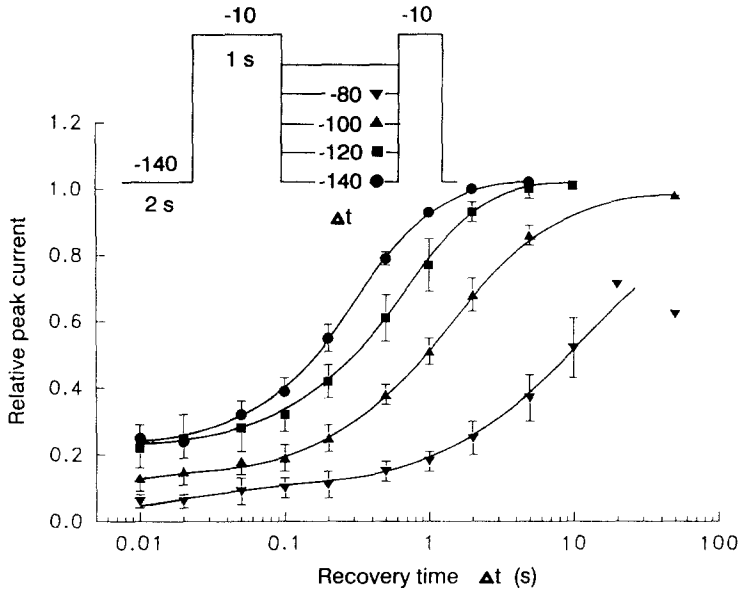

FIGURE 6. Recovery from inactivation in 5 mM $[K^+]_o$. Recovery was evaluated at holding potentials of −80, −100, −120, and −140 mV by the protocol displayed in the inset. The magnitude of the current elicited by the second depolarising pulse to −10 mV was compared to the magnitude of the first to assess the degree of recovery. Data from a total of six cells were normalized (see text) and averaged for each of the four holding potentials: −80 mV (▼, n = 3), −100 mV (▲, n = 5), −120 mV (■, n = 3) and −140 mV (●, n = 6). Error bars (± SEM) are shown when larger than symbol size. Lines through the points were drawn by eye. Points at 20 and 50 s represent single datum values from different cells.

inactivation of $I_K(t)$ by external K^+ ions. Evidence presented below strongly favors the second option.

If an additional K^+ current were activated, the tail currents may be expected to consist of both the rapid $I_K(t)$ tail current (as in Fig. 7 *A*) plus the longer duration tail current of the newly activated current. Tail currents in both normal and elevated $[K^+]_o$ generally consisted of the sum of two voltage-dependent exponential components. Time constants in both 5 and 25 mM $[K^+]_o$ were measured at −60 and −100 mV and are displayed in Table I. The Table I results indicate a clear increase in decay

time constants that cannot be explained by the superposition of an additional exponential component. Thus they suggest that external K^+ ions directly modify $I_K(t)$ deactivation kinetics.

In Fig. 7 *B*, it is clear that the increased $[K^+]_o$ also delayed activation kinetics. This was observed in one other cell, but unfortunately in both cases activation was not

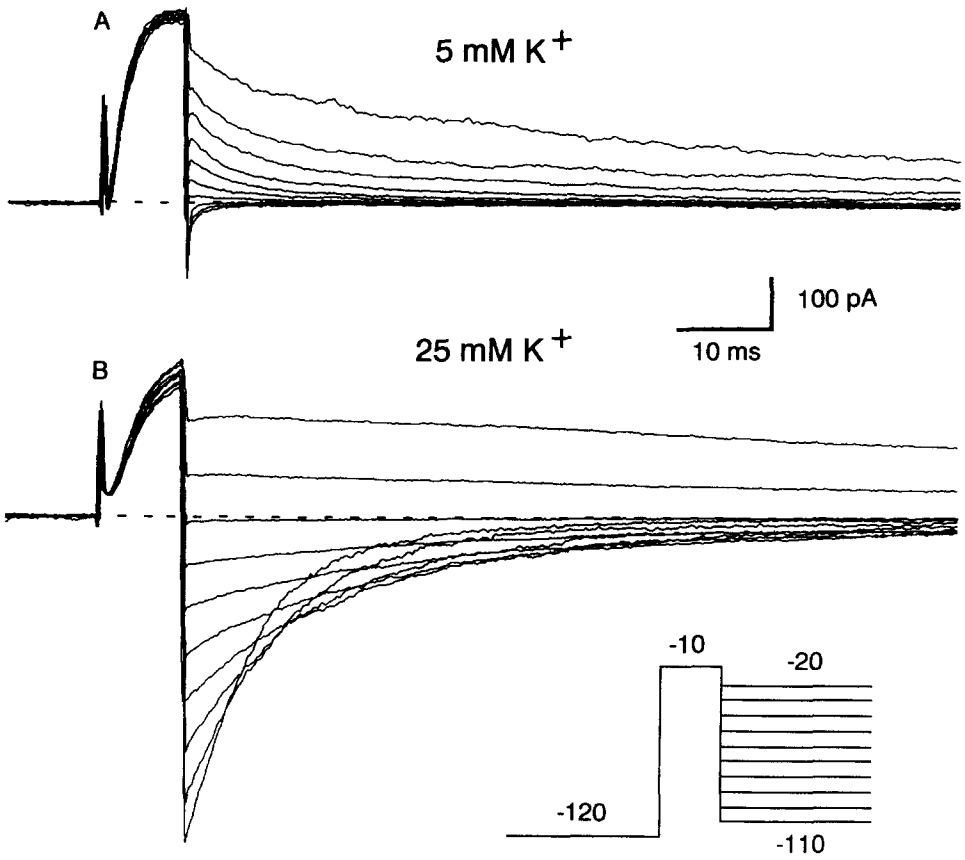

FIGURE 7. Tail currents elicited in 5 and 25 mM $[K^+]_o$ with external Na^+ replaced by choline. (*A*) Tail currents elicited in 5 mM $[K^+]_o$ by the voltage protocol shown in the inset. The reversal potential of $I_K(t)$ was −81 mV, close to the K^+ equilibrium potential of −82 mV. The dashed line is drawn through the steady-state current level for −80 mV. (*B*) The result of a similar experiment in the same cell bathed in 25 mM $[K^+]_o$. The reversal potential shifted to −39 mV, close to the K^+ equilibrium potential of −42 mV. Note the delay in both the activation kinetics and tail current deactivation kinetics induced by the elevated $[K^+]_o$.

examined over a wide range of potentials. However, in three other cells where time to one-half activation was measured between −30 and +40 mV, no change in the activation kinetics was noted when $[K^+]_o$ was increased from 5 to 25 mM (Fig. 4 *B*). Delays in activation kinetics seemed to occur in the cells expressing the proportion-

ately largest increases in deactivation time constants, but further clarification is required.

Inactivation kinetics of $I_K(t)$ were also significantly delayed in 25 mM $[K^+]_o$ (Fig. 8 *A*, cf. Fig. 2 *B*). The fast and slow time constants, which were constant between −10 and +40 mV, had mean values of 42 ± 1 and 250 ± 17 ms (both ± SEM, n = 12). These represent an increase by a factor of ≈ 2 times those measured in 5 mM $[K^+]_o$ solution. The transient component of this current was inactivated by a 1-s prepulse to −10 mV (Fig. 8 *B*).

If it is hypothesized that the intial peak current is predominantly $I_k(t)$ and that the current remaining after 500 ms represents a separate K^+ current activated by external K^+ ions, it may be anticipated that block by 4-AP will exert a differential effect on the early and late components of the total current. As indicated in Fig. 8 *C*, this was indeed the case. At +20 mV, 5 mM 4-AP reduced the peak current to 22% and the sustained current to 55%. However, this evidence may be misleading due to the nature of the block by 4-AP. Different inactivation rates of A currents have been shown to be due to single channels operating in different kinetic modes (Cooper and Shrier, 1989). Since 4-AP exerts its effect by interfering in a complex manner with

TABLE I

Fast (τ_f) and Slow (τ_s) $I_K(t)$ Deactivation Time Constants

	−100 mV		−60 mV	
	5 mM $[K^+]_o$	25 mM $[K^+]_o$	5 mM $[K^+]_o$	25 mM $[K^+]_o$
τ_f	0.8 ± 0.1 (n = 5)	2.6 ± 0.3 (n = 3)	3.9 ± 0.1 (n = 4)	14.0 ± 2.7 (n = 5)
τ_s	4.5 ± 0.4 (n = 5)	8.1 ± 1.0 (n = 5)	24.6 ± 3.5 (n = 5)	48.8 ± 9.1 (n = 5)

Tail currents were elicited as shown in Fig. 7. Time constants are given in ms ± SEM and were determined by the method shown in Fig. 4 *A*. In some cases (where n < 5), tail currents did not express a significant fast deactivation component.

channel gating machinery (Kasai et al., 1986; see also below), it is possible that the rapid and slow inactivation processes may be affected differently.

The steady-state inactivation of $I_K(t)$ in 25 mM $[K^+]_o$ was determined as described above. A typical result is given in Fig. 9 *A* (cf. Fig. 5 *B*). The averages from three cells are plotted in Fig. 9 *B*. Averaged currents at both the peak activation (■) and currents remaining between 450 and 500 ms later (□) were both measured and were found to have similar voltage dependences. The high $[K^+]_o$ solution also induced a −9 mV shift in the steady-state inactivation curve (Fig. 9 *B*, ■ and □) and a depolarization of at least 10 mV in the voltage dependence of current activation (●).

From this analysis, it appeared that the effect of increasing $[K^+]_o$ was to remove inactivation of $I_K(t)$, rather than to activate a discrete current. This conclusion is supported by (*a*) an increase in deactivation and inactivation time constants which cannot be explained by the superpositioning of an additional current and (*b*) the early and late components of the transient current having similar steady-state inactivation curves. It is also supported by single-channel data (see below).

Some evidence suggested that the elevated $[K^+]_o$ also activated a small persistent K^+ current, possibly distinct from the inactivating current discussed above. For

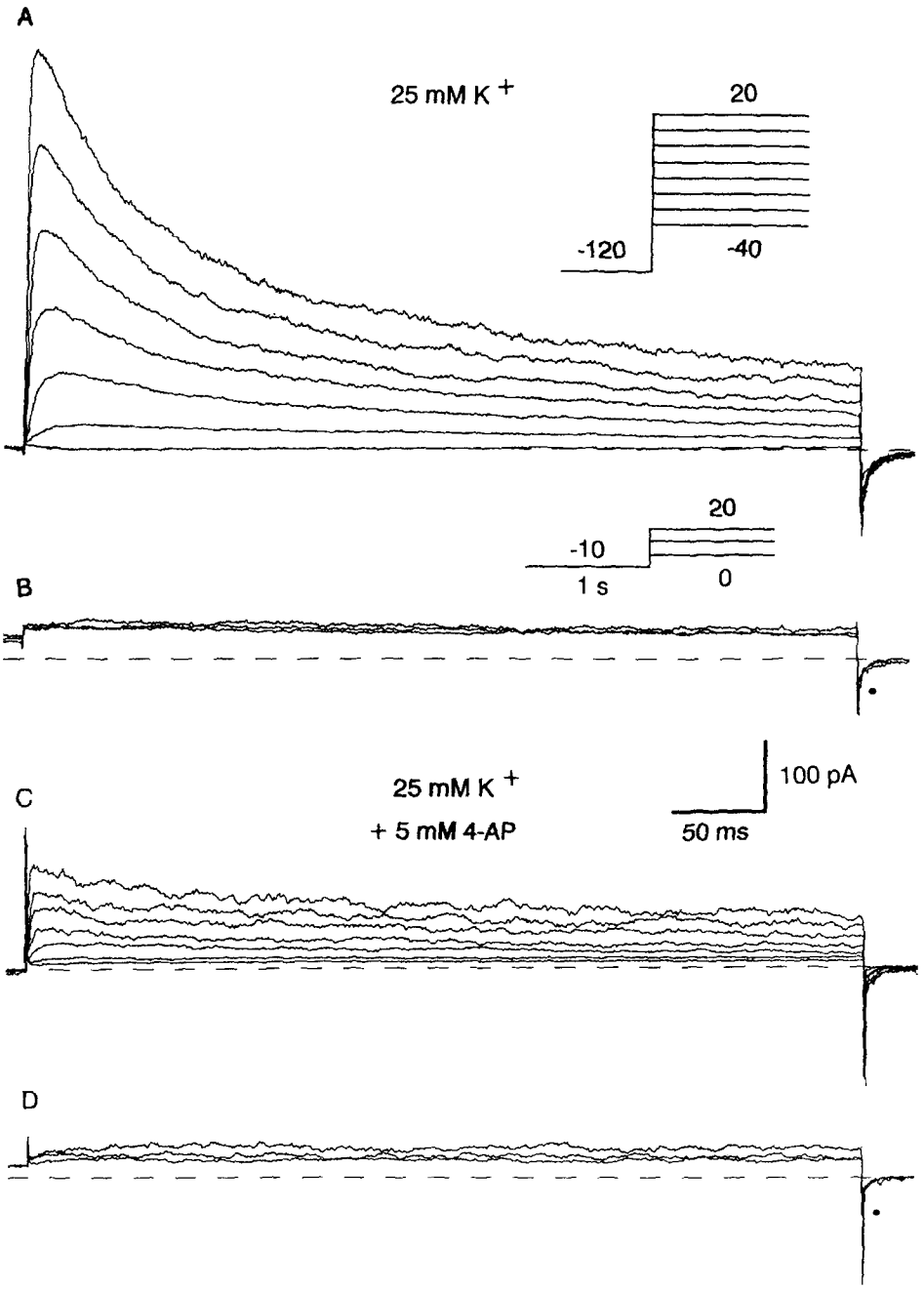

FIGURE 8. Currents activated in 25 mM $[K^+]_o$ by depolarization from negative holding potentials. Dashed lines are drawn through the steady-state current level for −80 mV. (*A*) Currents activated by stepping from −100 mV to potentials from −40 to +20 mV (10-mV increments). (*B*) Currents activated in the same cell at potentials of 0, 10, and 20 mV after 1-s prepulses to −10 mV. Note that tail currents of comparable time course persist (*dot*) despite the complete inactivation of the transient current. (*C*) The same experiment as shown in *A*, performed after adding 5 mM 4-AP to the external solution. 4-AP has a differential effect on early and late components of the current. Note the slight increase in linear leakage current. (*D*) Similar experiment as in *B* performed in 5 mM 4-AP. Note reduction of tail current amplitude (*dot*).

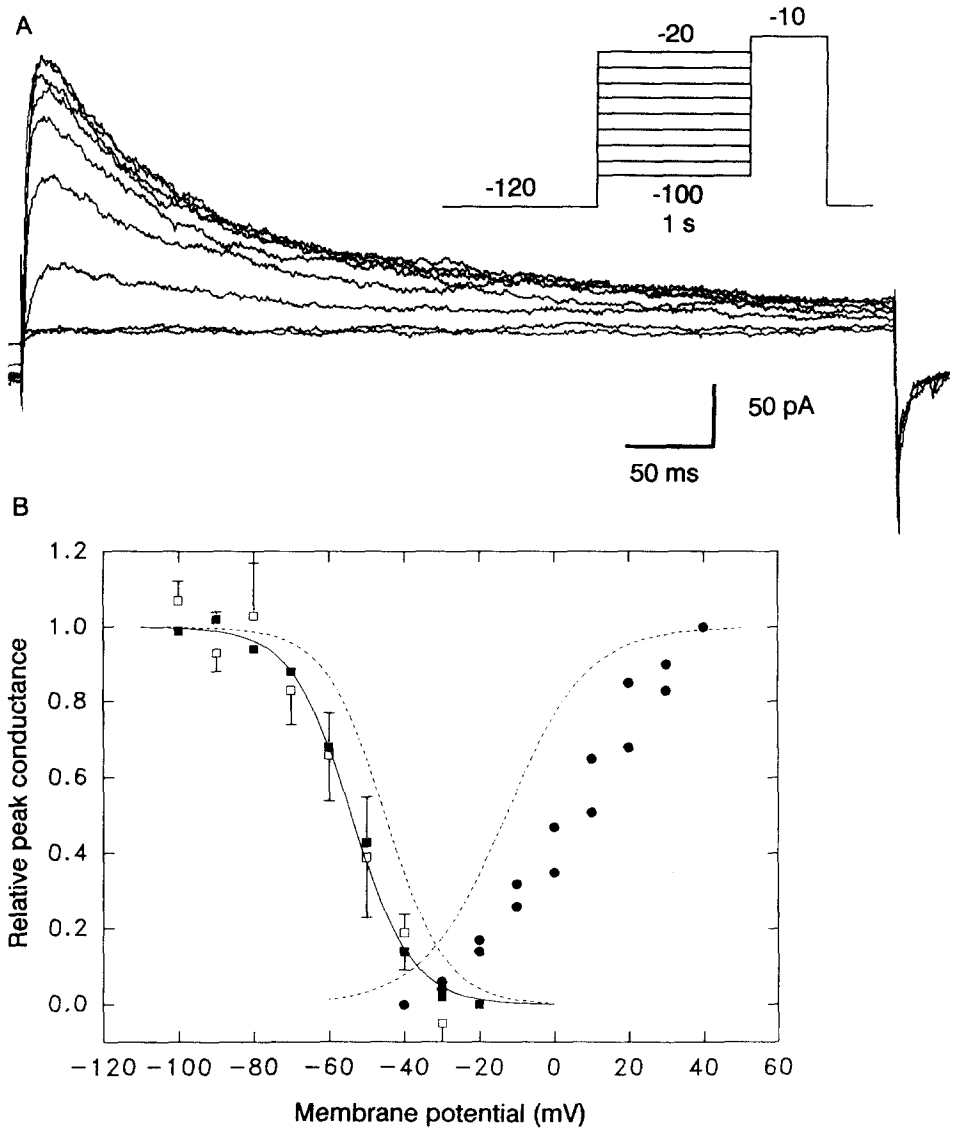

FIGURE 9. Steady-state inactivation and voltage-dependent activation in 25 mM $[K^+]_o$. (*A*) Example of inactivation data recorded from one cell by the voltage protocol illustrated in the inset. (*B*) Steady-state inactivation data measured from peak currents (■) and from currents averaged between 450 and 500 ms after depolarization (□), both averaged from the same three cells. Error bars (± SEM) are displayed when larger than symbol size. Currents elicited from −90 and −100 mV were averaged to determine maximum activation. The solid line represents a Boltzmann fit to data where V' is −54 mV. Peak activation conductance from two cells in 25 mM $[K^+]_o$ is also plotted (●). Conductances in each case were expressed as a fraction of those measured at +40 mV. Dashed lines represent the Boltzmann curves fitted to the inactivation and activation curves in 5 mM $[K^+]_o$ (from Fig. 5 *B*).

example, in Fig. 8 *B* (*dot*), when the transient component of $I_K(t)$ was completely inactivated, tail currents of a similar time course remained and were reduced in 5 mM 4-AP (Fig. 8 *D*, *dot*). These were not present in 5 mM $[K^+]_o$ (e.g., Fig. 2, *B* and *C*). Although too small to analyze quantitatively, these tail currents appeared to have similar kinetics to those elicited at peak current activation. Single-channel analysis clearly demonstrated that elevated $[K^+]_o$ not only delayed inactivation kinetics but also permitted a small amount of noninactivating current activity through the same channels.

Properties of Single Channels

Two types of transient K^+-selective channels were identified in single-channel recordings from the soma of these cells. Neither channel was affected by internal Ca^{++} concentration changes between submicromolar and millimolar levels. Channels were

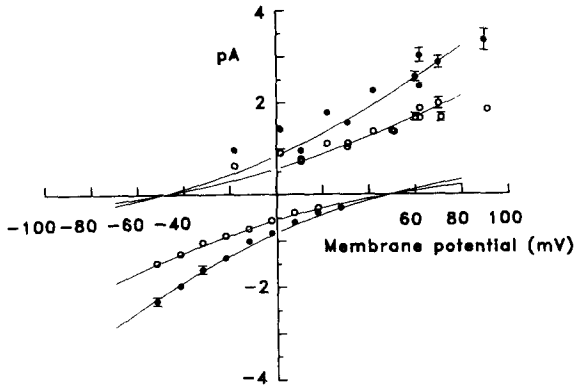

FIGURE 10. Current–voltage relationships for single transient K^+ channels. Inward currents (plotted in lower quadrants) were recorded from inside-out patches with high K^+ solution (145 mM $[K^+]_o$, 5 mM $[Na^+]_o$) in the pipette and GMR (5 mM $[K^+]_i$, 145 mM $[Na^+]_i$) in the bath. Points represent currents averaged from up to five cells and standard errors are shown when larger than symbol size. For inward currents, linear regression revealed single-channel conductances of 17 pS (○) and 26 pS (●). Outward currents were recorded from both inside-out and outside-out patches where the internal membrane surface was exposed to solutions containing 150 mM $[K^+]_i$ and 0 $[Na^+]_i$ and the external membrane was exposed to GMR. Points represent data averaged from single patches. The curves indicate the GHK equation fit to inward current data where $P_{Na}/P_K = 0.11$. The conductance of the larger channel (●) was 1.5 times that of the smaller channel. The slope conductances of these curves at −20 mV for inward current data were also 17 pS (○) and 26 pS (●).

distinguished by their different unitary conductances (Fig. 10) and kinetic behavior. The lower conductance channel was characterized by relatively longer mean open times and frequent rapid flickers to the closed state (Fig. 11). Several lines of evidence presented below suggest that both of these channels underlie $I_K(t)$.

Current–voltage relationships for both channels are plotted in Fig. 10. Inward currents were recorded from inside-out patches where the pipette contained 145 mM $[K^+]$ solution and the bath contained GMR. Outward currents were recorded either from inside-out patches, where the pipette contained GMR and the bath contained 150 mM $[K^+]$ solution, or from outside-out patches, where the pipette contained KF solution and the bath contained GMR. These data were fitted with the Goldman-

Hodgkin-Katz (GHK) current equation (Hodgkin and Katz, 1949):

$$I = I_K + I_{Na} = [P_K F^2 E/RT][C_o - C_i e^{-EF/RT}]/[1 - e^{-EF/RT}], \quad (5)$$

where

$$C_{o,i} = [K^+]_{o,i} + P_{Na}/P_K[Na^+]_{o,i}, \quad (6)$$

where I is the current, P_{Na} and P_K are the relative permeabilities of Na^+ and K^+, F is the Faraday constant, R is the universal gas constant, T is the absolute temperature,

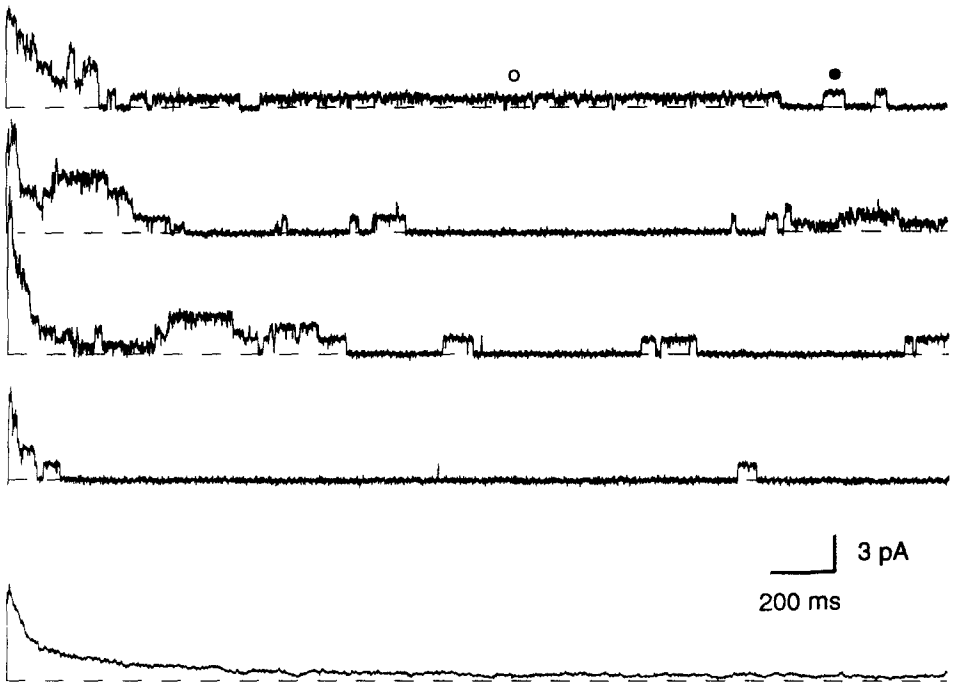

FIGURE 11. Activation of multiple transient K^+ channels. The patch was held at −110 mV (for 1 s) and outward currents were recorded in response to repeated depolarizations to +10 mV. The upper four traces are sequential and the ensemble average from 15 traces is shown below. This had inactivation time constants of 33 and 390 ms, plus a smaller longer component. The patch contained both channel types as indicated (○, 17 pS: ●, 26 pS). Data were recorded from an inside-out patch where the pipette contained GMR and the bath contained 150 mM $[K^+]$ solution.

and E is the membrane potential. If P_{Na}/P_K was assumed to be 0, the GHK equation gave a relatively poor fit to the inward current data. However, as shown in Fig. 10, the model provided a reasonable fit to these data when P_{Na}/P_K was assumed to be 0.11. Although it was shown earlier that $I_K(t)$ was very highly selective for K^+ (Fig. 7), in that case neither the internal nor the external solutions contained Na^+ ions. In Fig. 10, the slope conductances of the fitted curves for inward currents at −20 mV were 17 pS (○) and 26 pS (●), respectively. These were identical to the conductances

revealed by linear regression of the same points. However, linear regression revealed conductances of 14 and 23 pS, respectively, for outward currents. Inward current data were more reliable since most points (except those at the extremities) represented averages of at least 10 single-channel transitions from five different patches. The greater scatter in the outward current data is due mainly to the fact that each point represented data from a single patch and perhaps also to the slightly different ionic conditions between inside-out and outside-out patch recording configurations.

Single transient K^+ channels were observed in only ~20% of cell-attached patches, but many of these contained large numbers of both types of channels. In contrast to whole-cell currents which generally remained stable for the duration of the recording (often >30 min), single-channel activity often displayed rapid and irreversible rundown, sometimes disappearing completely after only a few depolarizations. We found that applying extra suction to a cell-attached patch, excising the patch, or exchanging the solution bathing an excised patch frequently accelerated the rate of channel rundown. The problems of channel lability and a propensity to form large clusters precluded quantitative analysis of single-channel kinetic properties.

An example of activation of transient K^+ channels is shown in Fig. 11. This was from an inside-out patch where the pipette contained Ringer's solution and the bath contained 150 mM [K^+] solution. Both the 17 and 26 pS channels were present. The ensemble average from 15 successive sweeps (during which little or no rundown occurred) displayed an inactivation time course that was described by the sum of two exponential components, with time constants of 33 and 390 ms, respectively. Another small inactivation component with a much longer time constant was also present.

The voltage dependence of channel activation was examined in two outside-out patches, each of which contained large numbers of channels. The membrane potential was held at −112 mV for 1 s, then stepped to voltages from −52 to +48 mV (20-mV increments) in a sequential manner so that the effects of rundown (if any) were evenly distributed. In any case, data were discarded whenever rundown appeared significant. Examples of averaged currents activated in one patch are given in Fig. 12 *A*. Normalized values of peak current amplitude from two patches are given in Fig. 12 *C*. The steady-state activation curve that was determined for whole-cell currents (*dotted line*) provided a reasonable fit to the data. The voltage dependence of steady-state inactivation was measured in one outside-out patch that contained multiple transient K^+ channels. The membrane potential was held at −112 mV for 2 s to reactivate a constant proportion of the channels. It was then stepped to voltages between −12 and −102 mV (10-mV increments) for 1 s and the availability of current was tested at +28 mV. Ensemble averages are displayed in Fig. 12 *B*. The voltage dependence of steady-state inactivation (Fig. 12 *C*) was closely approximated by the curve that was determined for the whole-cell current (*dotted line*). The steady-state inactivation and activation characteristics were only measured in patches containing both channel types. However, there did not seem to be significant differences in the voltage dependence of either type.

It is apparent from the data presented in Figs. 11 and 12 that single transient K^+ channels had a significant slowly inactivating component that was not clearly identified in whole-cell recordings. In each of seven patches (three inside-out and

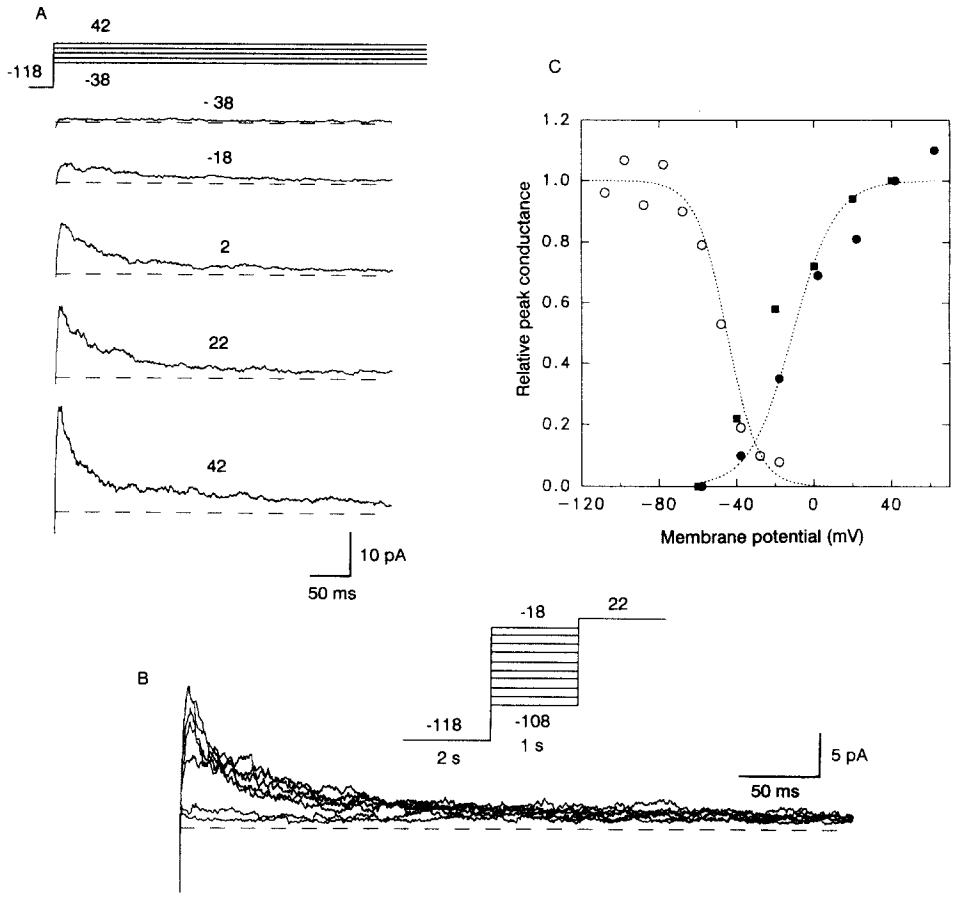

FIGURE 12. Voltage-dependent activation and steady-state inactivation of transient K^+ channels. (*A*) Ensemble averages of multiple K^+ channels from the same cell depolarized to potentials of −38, −18, +2, +22, and +42 mV from a holding potential of −118 mV (1 s). Dashed lines represent the current baseline. Note the small slowly inactivating component. Data were recorded from an outside-out patch where the pipette contained KF solution and the bath contained GMR. (*B*) An example of steady-state inactivation of multiple single transient K^+ channels. Ensemble averages activated upon depolarization to +22 mV from holding potentials of −18, −28, −38, −48, −58, −68, −78, and −98 mV are displayed. Voltage was held for 1 s at each holding potential, and was hyperpolarized to −118 mV for 2 s between test depolarizations (see *inset*). Currents activated upon depolarization from −88 and −108 mV are not shown, but are plotted in *C*, above. Data were obtained from an outside-out patch using similar solutions as in *A*. (*C*) Activation data from two outside-out patches (●, ■) with conductances normalized to near +40 mV. (●) Data shown in *A*. (○) Steady-state inactivation data for the data displayed in *B*. Dotted lines represent the steady-state inactivation and activation curves that were fitted to whole-cell currents in Fig. 5 *B*.

four outside-out) exposed to 5 mM $[K^+]_o$, this activity was observed to inactivate to negligible levels within 20–30 s. Transient K^+ currents with components that decay over similar time courses have been reported in other single-channel studies (Kasai et al., 1986; Cooper and Shrier, 1989). However, because of its small magnitude ($< 10\%$ of peak current), it was not clearly resolved in whole-cell recordings.

The effects of 5 mM 4-AP on single channels activated by depolarization were examined in six patches. In each case it reduced the amplitude of both the 17 and 26 pS channels by 20% and reduced channel open times by 50–80% (Figs. 13 *A* and 14). A further effect was to increase the duration of quiescent periods between bursts of channel activity. The effects were reversible (Fig. 14) and were similar to those reported for A channels in guinea pig dorsal root ganglion neurons (Kasai et al., 1986). The effect of 4-AP was tested only on the exposed surface of inside-out patches, whereas in whole-cell recordings it was applied to the external membrane. The similarity of its effect can be attributed to the fact that 4-AP readily permeates cell membranes. The application of 5 mM TEA to the external membrane of an outside-out patch reduced the unitary conductance of both channel types and appeared to prolong channel open times (Fig. 13 *B*).

The effects of increased $[K^+]_o$ on single-channel behavior were examined by two methods. First, the $[K^+]_o$ bathing the exposed surface of an outside-out patch was increased from 5 to 25 mM. Although solution exchange resulted in the irreversible rundown of a large proportion of the channels, the example shown in Fig. 13 *C* clearly indicates that inactivation was partially removed. Because of the difficulty in obtaining outside-out patches, the effect of increased $[K^+]_o$ was also examined on inside-out patches. In this case, transient K^+ channel activity in inside-out patches where the pipette contained 145 mM $[K^+]_o$ was compared with activity in other patches (both inside-out and outside-out) where the external membrane surface was exposed to 5 mM $[K^+]_o$. Because of the large variation in channel inactivation characteristics (Cooper and Shrier, 1989) and the inability to exchange solutions and thereby compare results from the same patch, the criterion of "noninactivating" channel activity was used as a basis for comparison. Noninactivating activity was defined as that present > 60 s after the previous depolarization. As stated above, when exposed to 5 mM $[K^+]_o$ the activity invariably declined completely within 30 s of a depolarization ($n = 7$), even in patches containing large numbers of channels. On the other hand, channels exposed to 145 mM $[K^+]_o$ displayed a much greater degree of slowly inactivating and noninactivating activity, even in patches containing few active channels. In 145 mM $[K^+]_o$, noninactivating activity was observed in 15/17 patches containing one to three active transient K^+ channels. It was observed for both channel types (17 pS, 11 patches; 26 pS, 6 patches). In addition, spontaneous activity was always accompanied by voltage-activated activity of a channel with identical conductance, strongly suggesting the channels were the same. An example of voltage-activated and noninactivating behaviour in a patch containing two 17 pS channels is shown in Fig. 14. Note that the noninactivating behavior was not continuous at the level displayed, but occurred in bursts lasting for several seconds separated by long periods (5–60 s) of quiescent activity. The fact that 5 mM 4-AP blocked both the voltage-gated and noninactivating channel activity ($n = 4$ patches) provides further evidence that they represent the same channels. Slowly inactivating

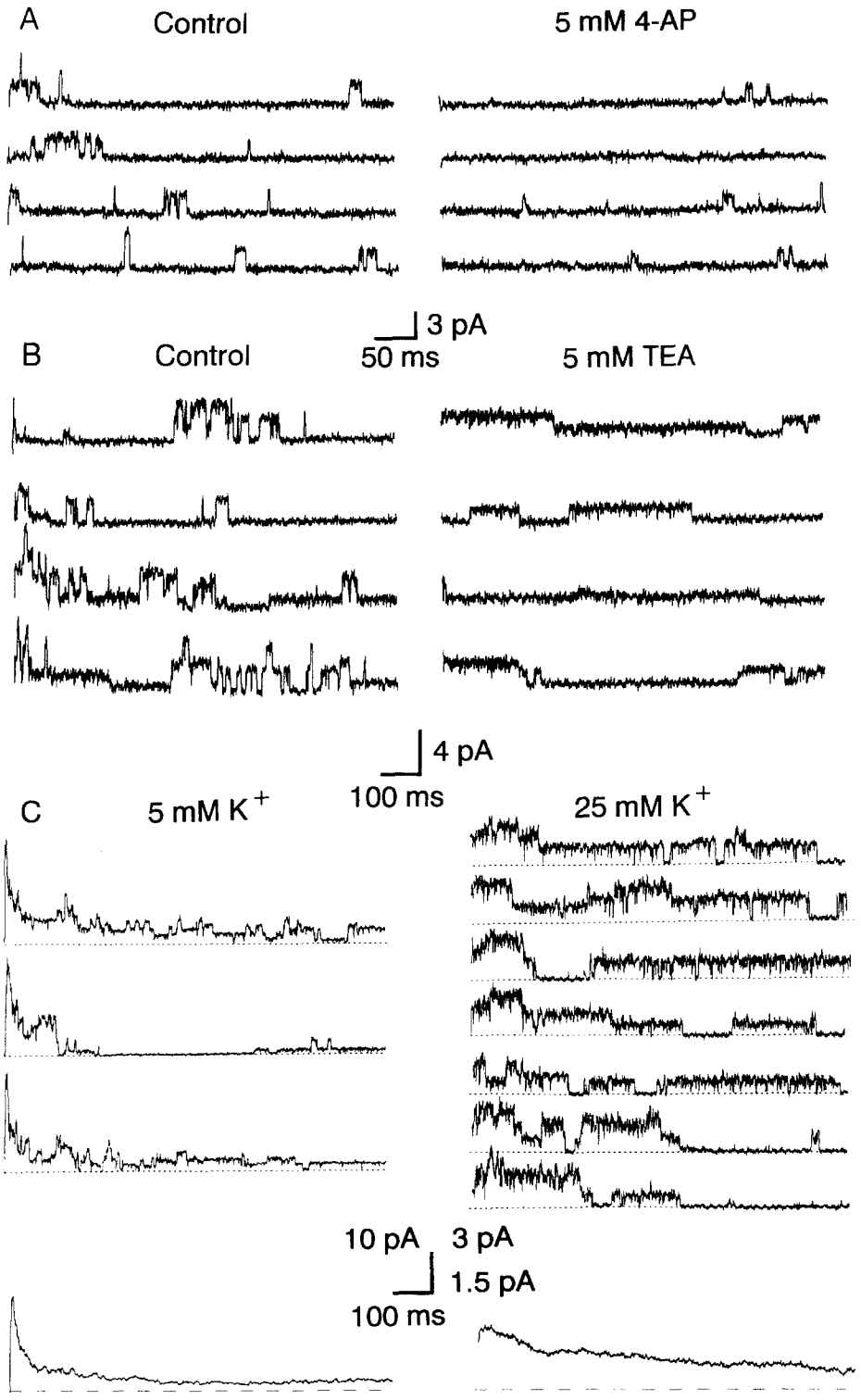
A
Control
5 mM 4-AP
3 pA
50 ms
B
Control
5 mM TEA
4 pA
100 ms
C
5 mM K+
25 mM K+
10 pA
3 pA
1.5 pA
100 ms

FIGURE 13.

and noninactivating activity was also invariably observed in patches containing large numbers of channels. Although noninactivating activity has only been demonstrated in 145 mM $[K^+]_o$, it is possible that it was also present in 25 mM $[K^+]_o$, as suggested by the tail currents that remained after complete inactivation of $I_K(t)$ (Fig. 8, *B* and *D*, *dots*).

DISCUSSION

Whole-Cell Resistance

The results presented here suggest that rat olfactory receptor neurons have an input impedance (R_o) of 20–30 GΩ in solutions where Na^+ has been replaced by choline. Although cells with visible cilia were preferentially selected for study, it is possible that measured values of R_o may have been enhanced by the partial loss of cilia. In determining R_o, it was assumed that the resting conductance was carried exclusively by K^+ ions. Na^+ current inactivation is completely removed at holding potentials more negative than −120 mV and the midpoint of the steady-state inactivation is ~−110 mV (Rajendra, Lynch, and Barry, unpublished). Activation of the Na^+ current is significant at −70 mV (Fig. 2 *A*). These factors imply a resting potential of ≤−90 mV, based simply on the ability of these cells to generate action potentials. This value is similar to the more negative resting potentials reported for amphibian olfactory receptor neurons (−90 mV in Frings and Lindemann, 1988) and virtually precludes significant resting Na^+ or nonspecific cation permeabilities, which would tend to depolarize the cell.

Comparison with Transient K^+ Currents in the Olfactory Receptor Neurons of Other Species

The characteristics of $I_K(t)$ are consistent with the limited information that has emerged from studies on amphibian cells. The current was first isolated in sala-

FIGURE 13. (*opposite*) Effect of 4-AP, TEA, and 25 mM $[K^+]_o$ on transient K^+ channels. In each case, the voltage step had just been completed at the start of the sweep. (*A*) Effect of 5 mM 4-AP on 26-pS channels. Currents were recorded at +46 mV after depolarization from −104 mV in an inside-out patch where the pipette contained GMR and the bath contained 150 mM $[K^+]$ solution. 4-AP was added to the bath. (*B*) Effect of 5 mM TEA on 17- and 26-pS channels. Data were recorded in response to depolarizations from −32 to +28 mV. The low holding potential was used to minimize the number of channels activated. Currents were recorded in an outside-out patch where the pipette contained KF solution and the bath contained GMR. TEA was added to the external membrane surface. (*C*) Effect of increasing $[K^+]_o$ on channel inactivation. The left panel shows three traces recorded after depolarisation of an outside-out patch from −112 mV (1 s) to +28 mV. The ensemble average (n = 9) is shown below. The pipette contained KF and the bath contained GMR. The right panel shows representative traces from the same patch after $[K^+]_o$ was increased to 25 mM. The ensemble mean of 46 traces is shown below. Identical voltage pulse protocols were used throughout the experiment. Note the different vertical scales. The 10-pA scale applies to all data (including ensemble average) in the left panel. The 1.5-pA scale applies to ensemble average trace on the right panel and the 3-pA scale applies to all traces above it.

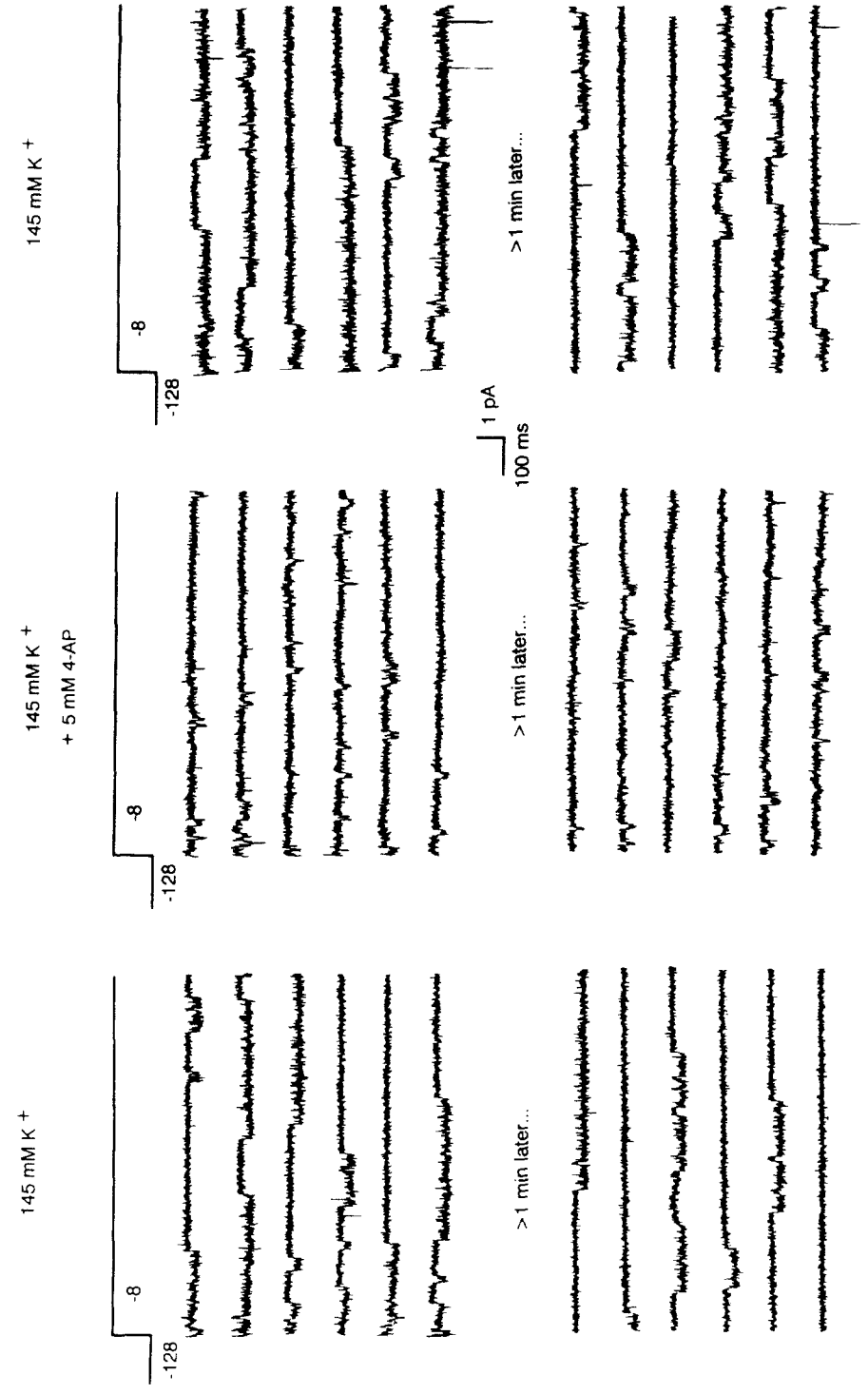
145 mM K +
-8
-128
>1 min later...
145 mM K +
+ 5 mM 4-AP
-8
-128
>1 min later...
145 mM K +
-8
-128
>1 min later...
1 pA
100 ms

FIGURE 14.

manders by Firestein and Werblin (1987*a*), who reported an inactivation time constant of 45 ms, roughly consistent with that reported here. Schild (1989) found that the steady-state inactivation of a transient K^+ current was completely removed by −80 mV and that the current was not activated in the subthreshold range for action potential generation (see below). Firestein and Werblin (1987*b*) also recognized that the transient current in salamander neurons required an unusually long period (5 s) to recover from inactivation. However, a contrasting feature is that the transient K^+ current in frog cells is resistant to block by 20 mM TEA (Trotier et al., 1989), whereas this concentration is sufficient to completely block the transient K^+ current described in this study (not shown).

The absence of $I_K(t)$ in the olfactory receptor neurons of some species, e.g., mudpuppy in Dionne (1989); lobster in McClintock and Ache (1989); bullfrog in Suzuki (1989) may be due to interspecies variation. As discussed below, a major role for $I_K(t)$ is probably spike repolarization and each of the species lacking this current invariably had much larger, more rapidly activating delayed rectifiers which would be suitable for the same role.

Comparison with Transient K^+ Currents in Other Cells

In 5 mM $[K^+]_o$ solution, $I_K(t)$ inactivates with time constants of 22.4 and 143 ms and a small component of several seconds. This is similar to the recent detailed description of A current inactivation in rat nodose ganglion neurons (Cooper and Shrier, 1989) which also identified three inactivation time constants. Although transient K^+ currents are generally reported to inactivate monoexponentially (for review, see Rudy, 1988), reports of double exponential decays are not uncommon. For example, Akasu and Tokimasa (1989), Clark et al. (1988), Mayer and Sugiyama (1988), and Oxford and Wagoner (1989) have described transient K^+ currents which decay with time constants similar to the two faster ones described here. In addition, several other whole-cell and single-channel studies (Gustafsson et al., 1982; Kasai et al., 1986; Salkoff and Wyman, 1980; Solc et al., 1987) have revealed a very slowly inactivating phase, with a time constant in the order of seconds. However, the magnitude of this component may vary considerably between preparations (Solc et al., 1987).

The complexity of the processes underlying the recovery from inactivation is an interesting feature of $I_K(t)$. The current amplitude recovers as sigmoidal function of time (Fig. 6). This characteristic is difficult to model as a simple stochastic process

---

FIGURE 14. (*opposite*) Effect of 145 mM $[K^+]_o$ on single transient K^+ channel inactivation properties. All data were from the same inside-out patch which originally contained two 17 pS channels, but one dropped out during the first solution exchange. The pipette contained 145 mM $[K^+]$ solution and the bath contained either GMR (*left and right panels*) or GMR + 5 mM 4-AP (*center panel*). All data were recorded at −8 mV in response to depolarizations from −128 mV (1 s). This figure showsthe coexistence of noninactivating and voltage-activated activity of transient K^+ channels exposed to 145 mM $[K^+]_o$. The upper six traces in each panel show examples of voltage-activated channel activity. The lower traces, which are continuous for each panel, display a single "burst" of noninactivating activity recorded between 1 and 2 min after the last depolarization. Bursts were separated by extended periods (5–60 s) of quiescent activity.

and suggests that another type of process may also contribute. The inactivating K^+ current described by Oxford and Wagoner (1989) displayed remarkably similar behavior. Another unusual feature of $I_K(t)$ is that the inactivation and voltage dependence are modulated by changes in $[K^+]_o$. In particular, increasing $[K^+]_o$ hyperpolarises the steady-state inactivation curve and partially removes inactivation. Cahalan et al. (1985) noted a similar but less dramatic effect on K^+ current deactivation in T lymphocytes. Kawa (1987) also reported the removal of inactivation of a transient K^+ current in activated thrombocytes, but this was mediated by a different mechanism and was not reversible.

Properties of Single Channels

Channels were frequently grouped into large clusters which often displayed rapid and irreversible rundown, sometimes within the space of several successive depolarizations. This was in marked contrast to the whole-cell $I_K(t)$ which generally maintained a constant magnitude for the duration of the recording (often >30 min). A similar observation has been made on the transient K^+ current in GH_3 pituitary cells (Oxford and Wagoner, 1989) where it was suggested that patch excision may have disrupted an inner membrane surface or cytoskeletal component necessary for channel activation. Dialysis of a diffusible intracellular substance was unlikely to have caused rundown as this should also have affected the whole-cell current. As stated above, the application of extra suction to a cell-attached patch, patch excision or exchange of the solution bathing an excised patch frequently accelerated the rate of channel rundown. These observations are consistent with the idea that mechanical stress may disrupt an internal membrane-bound component necessary for channel activation.

Other studies have presented evidence for both the clustering of single transient K^+ channels (Premack et al. 1989; Taylor, 1987) and irreversible channel rundown in excised patches (Marty and Neher, 1985; Oxford and Wagoner, 1989). Several studies where rundown was not reported were performed on cell-attached patches (Cooper and Shrier, 1985, 1989; Kasai et al., 1986). We find rundown is least in this configuration, but were precluded from using it because of large errors that exist in the measurement of transmembrane potentials and single-channel conductances in very small cells (Lynch and Barry, 1989).

Channels had unitary conductances of 17 and 26 pS and several lines of evidence support our conclusion that they underlie $I_K(t)$. Both channels were K^+ selective and were activated transiently by step depolarizations of the membrane potential. Inactivation time constants could not usually be measured precisely, but for large channel clusters appeared similar to those determined for $I_K(t)$. The voltage dependence of steady-state inactivation and the threshold for current activation of channel clusters were consistent with those measured for $I_K(t)$. The effects of 4-AP, TEA, and increased $[K^+]_o$ were also similar for both single-channel and whole-cell currents.

The co-existence of two different transient K^+ channels in the same cell has also been reported in cardiac cells (Benndorf et al., 1987). Although we could not detect any differences in voltage dependence between the two channel types, the possibility of small differences cannot be ruled out. It was clear that the channels had different kinetic properties but it was not possible to investigate these in detail. The unitary conductances of 17 and 26 pS are in the same range as those described elsewhere for

transient K^+ channels. For example, others have reported conductances of 43 pS (Florio et al., 1990), 22 pS (Cooper and Shrier, 1989), 20 pS (Kasai et al., 1986), 18 pS (FK channel in Marty and Neher, 1985) and 16 pS (K_W channel in Hoshi and Aldrich, 1988). From the analysis of inward single-channel currents (Fig. 11 *B*), it appeared that both 17- and 26-pS channels had a small but significant permeability to Na^+ ($P_{Na}/P_K = 0.11$). A similar conclusion was reached by Taylor (1987), who measured $P_{Na}/P_K = 0.09$ for an A current in molluscan neurons. Florio et al. (1990) also postulated a significant Na^+ permeability for single transient K^+ channels in avian neurons. However, Kawa (1987) reported a P_{Na}/P_K of <0.03 for a transient K^+ current in newt thrombocytes, which is similar to those reported for some other types of K^+ channels (reviewed by Hille, 1984). The possibility that Na^+ may be permeable in a subset of transient K^+ channels requires further investigation.

Cooper and Shrier (1989) found that the conductance of single A channels varied according to the square root of $[K^+]_o$. An apparently similar effect on whole-cell currents was observed by Oxford and Wagoner (1989). We were unable to demonstrate such a relationship at the single-channel level despite varying $[K^+]_o$ between 5 and 145 mM. The conductance and rectifying properties of the channels were well explained by the asymmetrical $[K^+]$ gradients and the predictions of the constant field (GHK) equation (Fig. 10). An increase in $I_K(t)$ conductance of 20–30% was observed when $[K^+]_o$ was increased from 5 to 25 mM, but this may be explained by the removal of inactivation on peak current magnitude. Furthermore, no evidence of a dependence on $[K^+]_o$ is present in the single-channel data of Kasai et al. (1986), suggesting that this property may not be a general feature of transient K^+ channels.

A Physiological Role for $I_K(t)$

Transient K^+ (or A) currents in other cells have several functions including regulation of the rate of repetitive firing (Connor and Stevens, 1971), control of cell excitability (Gustaffson et al., 1982) and modification of the shape and efficiency of excitatory junction potentials (Daut, 1973; Cassell and McLachlan, 1986). These functions depend on the ability of the current to activate in the voltage range between the resting potential and the threshold potential for action potential initiation. However, $I_K(t)$ has a significantly higher threshold for activation than the Na^+ current (Fig. 2 *A*), which effectively precludes its involvement in these roles. The high activation threshold implies an important role in spike repolarization, especially since $I_K(t)$ is larger and activates more quickly than the delayed rectifier.

Since $I_K(t)$ inactivates rapidly (within 50 ms) and recovers very slowly (50 s at -100 mV), such inactivation will accumulate with successive spikes and the ability of $I_K(t)$ to repolarize the cell will progressively diminish. This would lead to the progressive decrement of spike amplitude that is characteristic of olfactory receptor neuronal spike bursts (e.g., Trotier et al., 1989).

A physiological role for the removal of inactivation induced by increasing $[K^+]_o$ remains a matter for speculation. It is likely that given the existence of channel clusters and a restricted extracellular space, that high-frequency repetitive spiking will produce localized elevations in $[K^+]_o$. This would have the effects of partially removing $I_K(t)$ inactivation, reducing peak outward current flow (owing to a diminished K^+ concentration gradient and a shift in voltage dependence) and may also

delay $I_K(t)$ activation kinetics and depolarize the cell. Taken together, these effects could contribute to the progressive attenuation of spike amplitude and the elongation of action potential waveforms (Trotier et al., 1989), spike frequency adaptation (Getchell, 1986), and burst termination (Frings and Lindemann, 1988).

It may be relevant that the olfactory mucus contains an elevated $[K^+]$ (10 mM) and that this can be altered by odorant stimulation (Joshi et al., 1987). However, many channels are on the soma, which is not exposed to the mucus and it is not known whether the basolateral $[K^+]_o$ can also be modulated by odorants. This mechanism offers a possible means by which olfactory supporting cells could modulate the neuronal response.

Elevation of $[K^+]_o$ induced by action potentials has been demonstrated in the turtle olfactory nerve (Eng and Kocsis, 1987) and has been postulated to be important for olfactory transduction (Gesteland, 1988). The existence of $I_K(t)$ on olfactory nerve axons has not been proved, but evidence for clustered transient K^+ channels exist for at least some types of axons (Premack et al., 1989; Roper and Schwartz, 1989). It remains to be shown whether external $[K^+]_o$ can be modulated sufficiently to affect either somatic or axonal $I_K(t)$ kinetics and hence cell firing properties.

We thank Dr. Chris French for useful discussions. The financial support of the Australian Research Council and the National Health and Medical Research Council of Australia during the course of this work is also gratefully acknowledged.

Original version received 8 June 1990 and accepted version received 15 October 1990.

REFERENCES

Akasu, T., and T. Tokimasa. 1989. Potassium currents in submucous neurons of guinea-pig caecum and their synaptic modification. *Journal of Physiology.* 416:571–588.

Barrett, J. N., K. L. Magleby, and B. S. Pallotta. 1982. Properties of single calcium-activated potassium channels in cultured rat muscle. *Journal of Physiology.* 331:211–230.

Barry, P. H., and J. W. Lynch. 1991. Topical review. Liquid junction potentials and small cell effects in patch-clamp analysis. *Journal of Membrane Biology.* In press.

Barry, P. H., and N. Quartararo. 1990. PNSCROLL, a software package for graphical interactive analysis of single channel patch clamp currents and other binary file records: under mouse control. *Computers in Biology and Medicine.* 20:193–204.

Benndorf, K., F. Markwardt, and B. Nilius. 1987. Two types of transient outward currents in cardiac ventricular cells of mice. *Pflügers Archiv.* 409:641–643.

Cahalan, M. D., K. G. Chandy, T. E. DeCoursey, and S. Gupta. 1985. A voltage-gated potassium channel in human T lymphocytes. *Journal of Physiology.* 358:197–237.

Cassell, J. F., and E. M. McLachlan. 1986. The effect of a transient outward current (I_A) on synaptic potentials in sympathetic ganglion cells of the guinea-pig. *Journal of Physiology.* 374:273–288.

Clark, R. B., W. R. Giles, and Y. Imaizumi. 1988. Properties of the transient outward current in rabbit atrial cells. *Journal of Physiology.* 405:147–168.

Connor, J. A., and C. F. Stevens. 1971. Prediction of repetitive firing behaviour from voltage-clamp data on an isolated neurone somata. *Journal of Physiology.* 213:31–53.

Cooper, E., and A. Shrier. 1985. Single-channel analysis of fast transient potassium currents from rat nodose neurones. *Journal of Physiology.* 369:199–208.

Cooper, E., and A. Shrier. 1989. Inactivation of A currents and A channels in rat nodose neurons in culture. *Journal of General Physiology.* 94:881–910.

Daut, J. 1973. Modulation of the excitatory synaptic response by fast transient K^+ current in snail neurons. *Nature.* 246:193–196.

Deutsch, C., D. Krause, and C. Lee. 1986. Voltage-gated potassium conductances in human T lymphocytes stimulated with phorbol ester. *Journal of Physiology.* 372:405–423.

Dionne, V. E. 1989. Odor detection and discrimination: can isolated olfactory receptor neurons smell? *In* Chemical Senses. Volume 1: Receptor Events and Transduction in Taste and Olfaction. J. G. Brand, R. H. Cagan, J. H. Teeter, and M. R. Kare, editors. Marcel Dekker, Inc., New York. 415–426.

Eng, D. L., and J. D. Kocsis. 1987. Activity-dependent changes in extracellular potassium and excitability in turtle olfactory nerve. *Journal of Neurophysiology.* 57:740–754.

Firestein, S., and F. S. Werblin. 1987*a*. Gated currents in isolated olfactory receptor neurons of the larval tiger salamander. *Proceedings of the National Academy of Sciences.* 84:6292–6296.

Firestein, S., and F. Werblin. 1987*b*. Electrophysiological basis of the response of olfactory receptors to odorant and current stimuli. *Annals of the New York Academy of Sciences.* 510:287–289.

Florio, S. K., C. D. Westbrook, M. R. Vasko, R. J. Bauer, and J. L. Kenyon. 1990. Transient potassium currents in avian sensory neurons. *Journal of Neurophysiology.* 63:725–737.

Frings, S., and B. Lindemann. 1988. Odorant response of isolated olfactory receptor cells is blocked by amiloride. *Journal of Membrane Biology.* 105:233–243.

Gesteland, R. C. 1988. Receptor impulse interval patterns define equivalent olfactory stimuli. *Society for Neuroscience Abstracts.* 14:1062.

Getchell, T. V. 1986. Functional properties of vertebrate olfactory receptor neurons. *Physiological Reviews.* 66:772–818.

Gustafsson, B., M. Galvan, P. Grafe, and H. A. Wigstrom. 1982. A transient outward current in a mammalian central neuron blocked by 4-aminopyradine. *Nature.* 299:252–254.

Hamill, O. P., A. Marty, E. Neher, B. Sakmann, and F. J. Sigworth. 1981. Improved patch-clamp techniques for high-resolution current recording from cells and cell-free membrane patches. *Pflügers Archiv.* 391:85–100.

Hille, B. 1984. The Ionic Channels of Excitable Membranes. Sinauer Associates, Sunderland, MA. 426 pp.

Hodgkin, A. L., and B. Katz. 1949. The effect of sodium ions on the electrical activity of the giant axon of the squid. *Journal of Physiology.* 108:37–77.

Hoshi, T., and R. W. Aldrich. 1988. Voltage-dependent K^+ currents and underlying single K^+ channels in pheochromocytoma cells. *Journal of General Physiology.* 91:73–106.

Joshi, H., M. L., Getchell, B. Zielinski, and T. V. Getchell. 1987. Spectrophotometric determination of cation concentrations in olfactory mucus. *Neuroscience Letters.* 82:321–326.

Kasai, H., M. Kameyama, Y. Yamaguchi, and J. Fukida. 1986. Single transient K channels in mammalian sensory neurons. *Biophysical Journal.* 49:1243–1247.

Kawa, K. 1987. Transient outward currents and changes of their gating properties after cell activation in thrombocytes of the newt. *Journal of Physiology.* 385:189–205.

Kostyuk, P. G., O. A. Krishtal, and V. I. Pidoplichko. 1975. Intracellular dialysis of nerve cells: effect of intracellular fluoride and phosphate on the inward current. *Nature.* 257:691–693.

Lynch, J. W., P. H. Barry, and N. Quartararo. 1988. A temperature and solution control system for the measurement of single channel currents in excised membrane patches. *Pflügers Archiv.* 412:322–327.

Lynch, J. W., and P. H. Barry. 1989. Action potentials initiated by single channels opening in a small neuron (rat olfactory receptor). *Biophysical Journal.* 55:755–768.

McClintock, T. S., and B. W. Ache. 1989. Ionic currents and ion channels of lobster olfactory receptor neurons. *Journal of General Physiology.* 94:1085–1099.

Marty, A., and E. Neher. 1985. Potassium channels in cultured bovine adrenal chromaffin cells. *Journal of Physiology.* 367:117–141.

Maue, R. A., and V. E. Dionne. 1987*a*. Patch-clamp studies of isolated mouse olfactory receptor neurons. *Journal of General Physiology.* 90:95–125.

Maue, R. A., and V. E. Dionne. 1987*b*. Preparation of isolated mouse olfactory receptor neurons. *Pflügers Archiv.* 409:244–250.

Mayer, M., and K. Sugiyama. 1988. A modulatory action of divalent cations on transient outward current in cultured rat sensory neurons. *Journal of Physiology.* 396:417–433.

Oxford, G. S., and P. K. Wagoner. 1989. The inactivating K^+ current in GH_3 pituitary cells and its modification by chemical reagents. *Journal of Physiology.* 410:587–612.

Pixley, S. K., and R. Y. K. Pun. 1990. Cultured rat olfactory neurons are excitable and respond to odors. *Developmental Brain Research.* 53:125–130.

Premack, B. A., S. Thompson, and J. Coombs-Hahn. 1989. Clustered distribution and variability in kinetics of transient K channels in molluscan neuron cell bodies. *Journal of Neuroscience.* 9:4089–4099.

Roper, J., and J. R. Schwartz. 1989. Heterogeneous distribution of fast and slow potassium channels in myelinated rat nerve fibres. *Journal of Physiology.* 416:93–110.

Rudy, B. 1988. Diversity and ubiquity of K channels. *Neuroscience.* 25:729–749.

Salkoff, L., and R. Wyman. 1980. Facilitation of membrane excitability in *Drosophila. Proceedings of the National Academy of Sciences, USA.* 77:6216–6220.

Schild, D. 1989. Whole-cell currents in olfactory receptor cells of *Xenopus laevis. Experimental Brain Research.* 78:223–232.

Solc, C. K., N. Zagotta, and R. W. Aldrich. 1987. Single-channel and genetic analyses reveal two distinct A-type potassium channels in *Drosophila. Science.* 236:1094–1098.

Suzuki, N. 1989. Voltage- and cyclic nucleotide-gated currents in isolated olfactory receptor cells. *In* Chemical Senses Volume 1: Receptor Events and Transduction in Taste and Olfaction. J. G. Brand, R. H. Cagan, J. H. Teeter, and M. R. Kare, editors. Marcel Dekker, Inc., New York. 469–493.

Taylor, P. S. 1987. Selectivity and patch measurements of A-current channels in *Helix aspersa* neurons. *Journal of Physiology.* 388:437–447.

Trotier, D. 1986. A patch-clamp analysis of membrane currents in salamander olfactory receptor cells. *Pflügers Archiv.* 407:589–595.

Trotier, D., J.-F. Rosin, and P. MacLeod. 1989. Channel activities in *in vivo* and isolated olfactory receptor cells. *In* Chemical Senses Volume 1: Receptor Events and Transduction in Taste and Olfaction. J. G. Brand, R. H. Cagan, J. H. Teeter, and M. R. Kare, editors. Marcel Dekker, Inc., New York. 427–448.